

# Coke Quality Prediction Model Based on Coking Coal Group Composition and Structural Parameters and Its Coke Forming Mechanism

Weimao Song

Guangdong Jicheng Energy Chemical Co., Ltd, songwm@piscomed.com

**Abstract:** Taking five kinds of coking coal and 44 sets of coal blending as the research object, the coal cup coking experiment was completed in a 40kg small coke oven environment, and the coal heavy group, dense medium group and sparse coal obtained by separating the whole components of coal were obtained. The mass fraction YHC, YDMC, YLMC and the infrared spectral parameters I3 and I4 reflecting the hydrogen bond association and the length of the aliphatic chain or the degree of branching were the main indicators. The BP neural network analysis method was used to establish the coke quality prediction model. And discussed the characteristics of the model, and analyzed the coke formation mechanism under the new model. The results show that using new coal composition parameters to predict coke quality has certain advantages, and the predicted values (CSR), micro-strength (MSI), coke reactivity (PRI) and post-reaction strength (PSR) are measured and measured. The values are well consistent, and the fitting correlation coefficients for  $y=x$  are 0.986, 0.982, 0.956, and 0.926, respectively. The model has a good predictive effect on CR, MSI and PRI. The average deviation of the nine predicted samples is 0.53%, 1.58% and 1.28%, respectively. However, the PSR prediction effect after the reaction is poor, the average deviation At 12.22%. The research results provide a good basis for establishing a new method of coking coal blending.

**Keywords:** Coking coal blending; Coke quality; Forecast model; BP neural network; Coke formation mechanism

China's high quality coking coal reserves are limited. In order to save resources and meet coke quality requirements, coking enterprises generally use a variety of coal to coke with a certain proportion. Affected by regional and economic factors, the types and quantities of coal used by different enterprises may vary, and some may even reach more than 10 types <sup>[1]</sup>. The main factors affecting the quality of coke include the combination of coal properties and coking process, while the coking process and the properties of single coal can be determined. Therefore, optimizing the proportion of coal blending is an important way to obtain high quality coke and reduce production costs. In order to better guide coking coal blending, many scholars all over the world are committed to the establishment of scientific and accurate coke quality prediction models <sup>[2-6]</sup>. The establishment of the coke quality prediction model needs to consider two important factors: the selection of coal blending parameters and the choice of establishment methods.

Coal cohesiveness is an important property of coke formation of coal by pyrolysis <sup>[7,8]</sup>. The coke quality prediction in conventional coking coal blending usually considers coal cohesiveness as one of the important parameters, and the bonding index G or the maximum thickness of the colloidal layer is Y <sup>[9, 10]</sup>. However, both G and Y have certain disadvantages. For example, Y can only reflect the amount of colloidal bodies produced during coal pyrolysis and cannot make a reasonable judgment on the quality of colloidal mass, which often results in the different quality of coke produced by refining with similarity of Y <sup>[11]</sup>.

Although coal-rock blending as an advanced and mature theory has many applications, so far, there is no coal-rock blending method with universal significance and good effect <sup>[12,13]</sup>, based on any enterprise. The principle of coal and rock blending requires coking and coal blending to establish a new mathematical model from the beginning, and the process is difficult to promote. And no matter which coal-rock blending method pays too much attention to coal rock indicators and ignores some conventional coal quality indicators, it has one-sidedness.

The coking process is a complex production process with multiple parameters, time-varying, nonlinear and uncer

tainties, in which a series of complex physical and chemical changes occur, which are difficult to represent with a traditional, well-defined mathematical model. The back propagation network (BP network) has the characteristics of simple structure, strong fault tolerance and good controllability, and is widely used in engineering practice. Among them, the three-layer BP network can realize any continuous function with arbitrary precision when the middle layer unit is freely set according to the needs <sup>[14]</sup>, which is more suitable for the establishment of the coke quality prediction model. For example, Zhou Hong et al <sup>[15]</sup> used the linear weighted correction of coal blending index G, volatile matter V<sub>daf</sub>, sulfur fraction St, d and ash Ad as model input, with coke cold crushing strength M40 and wear resistance M10, Sulfur and ash were used as model outputs, and the coke quality prediction model was established by BP neural network. Liu Jun et al. <sup>[16]</sup> also used these parameters as the input and output of the model, and found that when the number of hidden layer neurons is 15, it is established. The BP neural network model has the best predictive effect on coke quality. Jiang Jing et al <sup>[17]</sup> proposed linear regression to predict coke ash and sulfur, while BP neural network predicted coke M40, M10, reactivity index CRI and post-reaction intensity. CSR, simulation results show that the prediction model has higher prediction accuracy and better adaptability.

In the previous research, our group found that the separation and extraction methods based on CS<sub>2</sub>/NMP solvent can separate the components of coal with different bonding ability and coking characteristics, so that the non-limousal angle is more accurate. It reveals the content and quality of the active component and the non-bonding inert component in coal <sup>[18]</sup>; further studies have found that the cohesive strength of coking coal and the FT-IR specific functional group absorption peak of the coal itself. There is a close relationship between them, which proposes two infrared parameters I3 and I4 that complement each other to determine the coal bondability, and explores the new mechanism of coal bond formation from the perspective of coal chemical structure <sup>[19]</sup>. Based on this, this study intends to construct a new set of coking coal blending parameters and combine BP network to study the new model of coke quality prediction, which will provide a basis for the establishment of a new coking coal blending method.

## 1. Experimental Part

### 1.1 Sample Preparation and Coal Quality Analysis

Five kinds of washed coking coals, Xinlei (XL), Bailong (BL), Yucheng (YC), Jinxing (JX) and Tianyi (TY) collected from a coking plant were selected as experimental coal samples. The samples used in the coal quality analysis and extraction back extraction experiments were sealed by a pulverizer to a bag of about 150 mesh and kept in an inert environment for standby; the coal samples for coal blending coking were broken up to a particle size of  $\leq 1.6$  mm for use. Coal sample industry analysis and elemental analysis are shown in Table 1.

Table 1 Proximate and ultimate analyses of coal samples

Coal sample	Proximate analysis $w/\%$				Ultimate analysis $w_{daf}/\%$				
	$M_{ad}$	$A_d$	$V_{daf}$	$FC_{daf}$	C	H	O <sup>*</sup>	N	S
XL	1.34	7.60	27.65	72.35	87.52	5.37	3.40	1.50	2.21
BL	0.82	8.95	32.67	67.33	86.52	5.52	5.54	1.61	0.81
YC	0.68	8.69	37.13	62.87	86.24	6.06	5.09	1.63	0.98
JX	1.90	11.16	36.21	63.79	84.25	6.08	7.25	1.68	0.74
TY	1.26	10.05	33.86	66.14	83.15	5.55	8.54	1.62	1.14

\* : by difference

### 1.2 Non-lithographic Phase Activity / Inert Component Separation

According to the method of <sup>[20]</sup>, the five coal samples were extracted and back-extracted with CS<sub>2</sub>/NMP (1:1, V/V) mixed solvent and stripping agent to separate the coal group components to obtain the coal heavy mass group (HC), dense medium group (DMC), thin medium group (LMC) and light group (LC) four major components. Literature <sup>[18]</sup> pointed out that there is a cohesive active component in coal. During the extraction and stripping process, the cohesive active component is naturally enriched in the dense medium group and the sparse medium group, wherein the dense medium group is for components with strong bonding ability, the medium-sized group is a component with weaker bonding ability, and the heavy group is a non-sticky component. Corresponding to and distinguishing the theory of coal and rock

coal blending, "The vitrinite group and the chitin group are active components, the silk group is an inert component, and the semi-vitram group is an amphoteric component" [12]. This study refers to the heavy group. It is a non-lithologic inert component, and the dense intermediate group and the thin medium group are non-lithographic active components. The dry ashless base yield of each family component is shown in Table 2.

Table 2 Yield of each group component after separation of all components

Sample	$w_{daf}/\%$				
	$Y_{DMC}$	$Y_{LMC}$	$Y_{HC}$	$Y_{LC}$	$\Delta L$
XL	11.46	20.48	65.33	0.71	2.02
BL	9.00	20.66	67.62	1.09	1.63
YC	11.94	26.79	59.15	1.27	0.85
JX	8.21	12.10	77.52	0.88	1.29
TY	5.65	12.59	79.38	1.29	1.09

$\Delta L$ : amount at stake

### 1.3 FT-IR Determination of Coal Samples

The samples were analyzed by Nicolet 6700 Fourier transform infrared spectrometer from Nicolet. The dried sample was mixed with spectrally pure KBr (1:100, mass fraction) and placed in an agate mortar. The sample and the carrier were ground and mixed uniformly, and then pressed and molded. The molded sheet was placed in the infrared spectrometer sample chamber for testing [21]. The spectral range is 4000-400 cm<sup>-1</sup>, the resolution is 4 cm<sup>-1</sup>, and each spectrum is cumulatively scanned 16 times.

### 1.4 Coal Blending Coking Experiment

The coal blending coke experiment was completed in a 40kg experimental coke oven. The process was as follows: a coal sample with a particle size of  $\leq 1.6$ mm was scaled to a self-made coal cup with a height of 70mm,  $\phi 67 \times 4.5$ mm and four  $\phi 3$ mm holes at the bottom. In the middle, stir with a stir bar for 3 min, flatten (at this time, the thickness of the coal seam is about 23.5 mm), then put the tablet and the compact (pressing piece  $\phi 66 \times 3$ mm, mass about 70g; the block height is 35mm,  $\phi 49.5$ mm, the quality is about 530g); transfer the coal cup to the coke oven, using a heating method to increase the furnace temperature from 700 °C to 1060 °C, heating time 2 h, heating rate 1 °C / min; wet cooling coke naturally drying After about 40 hours, it was transferred to a vacuum drying oven, dried at 105 °C for 3 hours, and bagged for use. The coal cups, briquettes, tablets and stir bars used in the experiment and the prepared coke are shown in Figure 1.

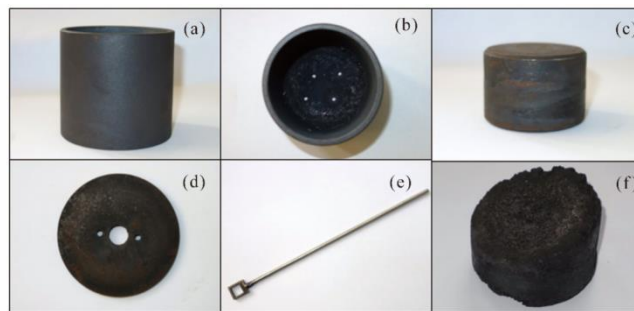


Figure 1 Coal blending coke experimental equipment and prepared coke

$G_{LMC} \times Y_{LMC}$  is used to indicate the ability of the viscous active component in the medium-sized group ( $G_{LMC}$  indicates the adhesion index G of the LMC component, the same below), and the ability of  $G_{DMC} \times Y_{DMC}$  to represent the adhesive active component in the dense medium group. The value, the capacity value of the inert component in the heavy group is represented by  $G_{HC} \times Y_{HC}$ , and it can be seen from Fig. 2 that there is a good correlation between the G value of the raw coal and  $G_{LMC} \times Y_{LMC} + G_{DMC} \times Y_{DMC}$ , and the  $R^2_{adj}$  reaches 0.95. Explain that the coal briquetting capacity can be

expressed by the active component capacity value. For this reason, when determining the blending ratio of the coal blending coking experiment, the  $G_{LMC} \times Y_{LMC} + G_{DMC} \times Y_{DMC}$  value is taken as a reference. Specifically, the coking experiment is carried out with each type of coal and two pairs of matching coals; for the coal blending, 6-7 mixing ratios are selected for each of the two single coal types; in order to make the mixture ratio uniform,  $G_{LMC} \times Y_{LMC} + G_{DMC} \times Y_{DMC}$  is taken as an indicator. For example, if YC and BL match, the  $G_{LMC} \times Y_{LMC} + G_{DMC} \times Y_{DMC}$  values of YC and BL are calculated to be 35.5 and 27.7, respectively, in [27.7, 35.5]. The six values of 29, 30, 31, 32, 33 and 34 are uniformly selected as the  $G_{LMC} \times Y_{LMC} + G_{DMC} \times Y_{DMC}$  values of the coal blended, and then the proportions of YC and BL in the blended coal are calculated separately. The coal blending scheme thus determined is shown in Table 3.

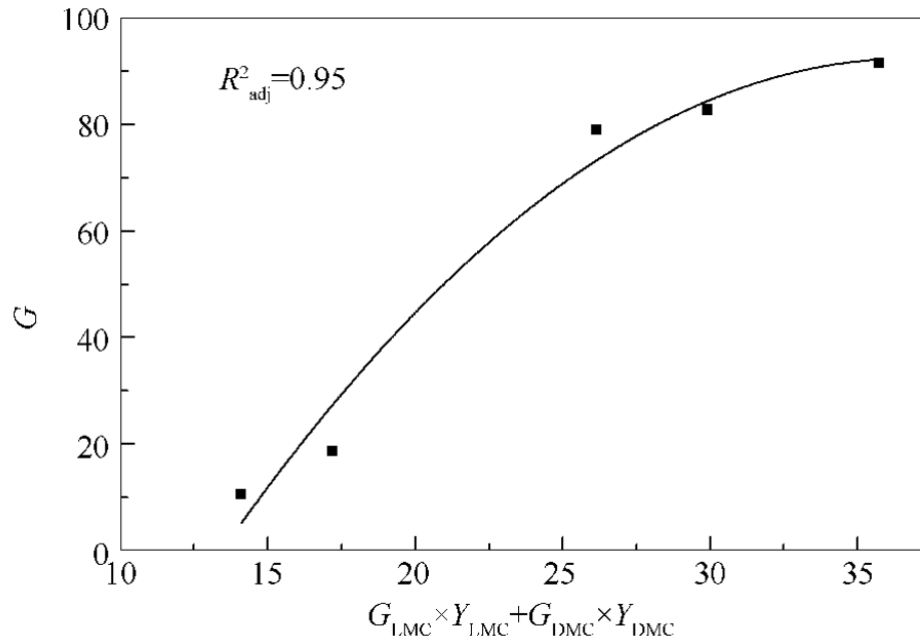


Figure 2  $G$  and  $G_{LMC} \times Y_{LMC} + G_{DMC} \times Y_{DMC}$

The coke formation and performance were characterized by four indexes: coke formation rate (CR), microscopic intensity (MSI), particle coke reactivity (PRI) [22] and post-reaction strength (PSR) [23]. Among them, the CR calculation is shown in formula (1), the MSI and PSR are measured by SYD-F200W coke micro-intensity meter (Anshan Xingyuanda Technology Co., Ltd.), and the PRI measurement is performed on the dynamic particle coke reactivity tester of North China University of Technology. The specific results are shown in Table 4.

$$CR = \frac{\text{Total dry coke quality}}{\text{Total mass of coal blended into the coal cup}} \times 100\% \quad (1)$$

Table 3 Ratio of each coal sample for coking experiment

No.	Ratio /%					No.	Ratio /%				
	XL	YC	BL	JX	TY		XL	YC	BL	JX	TY
1	100	—	—	—	—	26	—	69.61	—	30.39	—
2	—	100	—	—	—	27	—	53.14	—	46.86	—
3	—	—	100	—	—	28	—	36.67	—	63.33	—
4	—	—	—	100	—	29	—	25.69	—	74.31	—
5	—	—	—	—	100	30	—	14.71	—	85.29	—
6	81.83	—	—	18.17	—	31	—	87.57	—	—	12.43
7	66.50	—	—	33.50	—	32	—	72.85	—	—	27.15
8	51.18	—	—	48.82	—	33	—	58.14	—	—	41.86
9	43.52	—	—	56.48	—	34	—	43.42	—	—	56.58
10	28.19	—	—	71.81	—	35	—	33.61	—	—	66.39
11	12.87	—	—	87.13	—	36	—	23.80	—	—	76.20
12	84.42	—	—	—	15.58	37	—	13.99	—	—	86.01
13	71.28	—	—	—	28.72	38	—	—	83.53	16.47	—
14	58.15	—	—	—	41.85	39	—	—	73.90	26.10	—
15	51.58	—	—	—	48.42	40	—	—	64.28	35.72	—
16	38.44	—	—	—	61.56	41	—	—	45.03	54.97	—
17	25.31	—	—	—	74.69	42	—	—	27.07	72.93	—
18	14.29	—	—	—	85.71	43	—	—	6.54	93.46	—
19	—	80.38	19.62	—	—	44	—	—	86.37	—	13.63
20	—	67.60	32.40	—	—	45	—	—	70.46	—	29.54
21	—	54.81	45.19	—	—	46	—	—	54.54	—	45.46
22	—	42.03	57.97	—	—	47	—	—	38.62	—	61.38
23	—	29.25	70.75	—	—	48	—	—	22.71	—	77.29
24	—	19.28	80.72	—	—	49	—	—	14.75	—	85.25
25	—	86.08	—	13.92	—						

## 2. Selection of Coal Blending Parameters

Coal blending parameters commonly used to predict coke quality include volatiles Vdaf, sulfur St, d, ash Ad, alkalinity index MBI, mineral catalytic index MCI, basic fluidity MF, binder index G, and maximum colloidal layer thickness Y Etc [24, 25]. Among them, Vdaf can characterize the degree of coal metamorphism. Vdaf and Ad are closely related to the thermal properties of coke such as reactivity and post-reaction strength, and Vdaf and Ad have good additivity [25]. Therefore, Vdaf and Ad are retained as Coal blending quality parameters.

As mentioned above, the heavy group in coal is a non-lithologic inert component, and the dense medium group and the sparse middle group are non-lithologic active components, and their content (yield) is closely related to coal's bonding ability and cohesiveness related. The research of this group [15] pointed out that benzene series compounds, naphthalene series compounds, bismuth and phenanthrene series compounds and long-chain alkanes in coal are active components formed by coal bonding. The reason why the dense medium group has strong bonding ability is that it contains a large amount of adhesive active components in the group; the reason why the thin medium group has the bonding ability but weak ability is that the group component also contains a cohesive active ingredient but less possessed. These adhesive active components have moderate molecular structures (such as bridges, groups and heteroatoms that are easily combined with other components in coal, high aliphatic structures and phenol, alcohol, amine structures) and sizes (belonging to medium size molecular), which mainly produces a colloidal liquid phase during pyrolysis, and the resulting liquid phase has very good cross-linking points and bonding points; the amount of liquid phase depends on the level of the binding active component contained in the two components; while the heavy group component has a macromolecular structure, which mainly produces gas phase, tar vapor and solid phase during pyrolysis, and does not produce liquid phase. Or the liquid phase is very small, so it can not produce good adhesion, but the good effect between it and the liquid phase can also affect the coal bond size. Pyrolysis experiments on family components [26], the Shuzhong Formation is the main source of coal pyrolysis expansion, the Mizhong Formation is the main source of coal pyrolysis fluidity, and the heavy group is hot. Swelling and fluidity are hardly provided during the solution process.

Therefore, the selection of  $Y_{DMC}$ ,  $Y_{LMC}$  and  $Y_{HC}$  as the coal quality index of coal blending can not only reflect the content of the cohesive active and inert components in coal from the coal chemical composition and structure, but also reflect the coal pyrolysis process. The ability to flow and expand. The yield of the various components of the coal blending can be obtained by adding the corresponding yields of the individual coals.

Table 4 Coke performances

No.	CR/%	MSI/%	PRI/%	PSR/%	No.	CR/%	MSI/%	PRI/%	PSR/%
1	71.98	48.28	61.16	21.88	26	65.51	38.06	52.25	49.98
2	54.94	27.93	57.50	23.15	27	67.20	51.77	56.05	52.90
3	66.15	49.80	58.80	17.51	28	67.58	46.21	57.63	46.96
4	67.31	47.51	59.79	44.64	29	66.71	46.47	60.30	40.70
5	70.40	43.56	60.87	44.77	30	67.63	46.89	59.15	42.29
6	72.93	45.21	57.35	33.65	31	57.86	37.37	61.97	15.94
7	72.50	45.03	58.06	35.96	32	63.64	44.97	62.80	13.16
8	71.48	51.81	56.94	45.59	33	68.82	50.96	60.92	23.95
9	70.94	50.95	59.03	37.81	34	69.93	44.23	63.72	21.55
10	70.26	50.73	61.85	31.61	35	69.26	42.33	63.40	31.02
11	69.45	43.53	62.55	37.49	36	70.28	39.37	67.37	23.10
12	71.42	40.48	65.07	27.50	37	71.88	39.71	71.66	20.40
13	72.84	43.74	62.65	29.56	38	69.60	45.24	57.90	26.35
14	72.83	45.70	53.13	51.78	39	69.27	44.28	61.46	16.76
15	72.63	41.63	63.00	28.26	40	68.65	49.76	58.22	30.51
16	71.94	47.30	55.37	46.54	41	69.82	50.40	60.10	30.56
17	72.36	50.44	65.00	32.41	42	69.77	48.02	59.32	40.63
18	70.92	41.85	66.13	28.68	43	69.92	42.64	63.05	34.02
19	55.77	30.18	60.13	15.35	44	68.35	44.30	60.95	20.13
20	64.04	38.43	60.35	20.78	45	71.55	48.73	62.84	25.12
21	61.71	41.42	52.60	34.37	46	73.31	49.32	63.12	30.40
22	65.70	36.04	58.20	17.30	47	71.91	41.33	67.00	17.87
23	65.03	39.81	57.35	14.97	48	72.45	40.52	73.08	15.30
24	62.86	33.89	61.56	39.04	49	71.92	41.26	69.93	19.46
25	61.93	33.51	59.50	22.37					

Coal bonding is the main basis for evaluating the use of bituminous coal for coking. The bonding index G and the maximum colloidal layer thickness Y are commonly used indicators for characterizing coal adhesion. However, the coal bond formation mechanism is complicated. The existing adhesion evaluation methods generally refer to the coal as a whole, and do not reflect the origin of the bond from the coal composition structure. And the bond index G does not have additive; although Y has additive properties, it can only reflect the number of colloids, but not the quality of colloids [27]. Therefore, it is necessary to find new indicators that can characterize coal cohesiveness from the viewpoint of coal composition structure and have additive properties.

Our research group found that the relationship between the functional group structure of the infrared spectrum of coking coal and its adhesion is found [19], reflecting the hydrogen bond association in coal and the length of the fat chain or the degree of branching I3 and I4 (see (2) and (3)). The two parameters complement each other to determine the coal bondability. Among them, the aliphatic structure is the only decisive factor for the formation of coal bond, and the hydrogen bond association structure containing -OH (or -NH) is used as an aid. Factors can interact with the fat chain in coal bonding. Since parameters I3 and I4 express the characteristic information of coal in composition and structure, reflecting the essential factors of coal bond formation, the infrared spectral parameters I3 and I4 of coal are selected as new indicators to characterize coal adhesion. The coal blending is a physical mixing by a single coal, and the physical mixing does not cause a change in the functional group structure in the coal [28]. Therefore, I3 and I4 are also additive.

$$I3=P3700-3000/P1600(2)I4=(P2920/P2950)/P1600(3)$$

Therefore,  $Y_{DMC}$ ,  $Y_{LMC}$ ,  $Y_{HC}$ ,  $V_{daf}$ ,  $Ad$ ,  $I3$  and  $I4$ , as the coal blending parameter required to establish the coke quality prediction model, the corresponding value of the coal blended is calculated from the corresponding index of the single coal, and the calculation formula is as shown in formula (4). See Table 5 for the quality parameters of coal blending.

$$Ti=\sum Xj \times Tij(4) \text{ where } Ti: \text{ the } i\text{-th technical index of coal blending, } i=1, 2, 3, \dots, m \text{ (this article } m=7\text{); } Xj: \text{ the ratio}$$



of the jth single coal, %,  $j = 1, 2, 3, \dots, n$ ;  $T_{ij}$ : the i-th technical index of the j-th single coal.

Table 5 Quality parameters for blended coals

No.	Quality parameters for blended coals						
	$Y_{DMC}/\%$	$Y_{LMC}/\%$	$Y_{HC}/\%$	$V_{daf}/\%$	$A_d/\%$	$I_3$	$I_4$
1	11.46	20.48	65.33	27.65	7.60	22.69	2.61
2	11.94	26.79	59.15	37.13	8.69	15.03	2.15
3	9.00	19.66	63.62	32.67	8.95	18.66	2.63
4	8.21	12.1	77.52	36.21	11.16	16.97	3.13
5	5.65	12.59	79.38	33.86	10.05	5.86	2.95
6	10.87	18.96	67.55	20.44	8.25	21.65	2.61
7	10.37	17.67	69.41	21.36	8.79	20.77	2.62
8	9.87	16.39	71.28	22.28	9.34	19.90	2.62
9	9.62	15.75	72.22	22.74	9.61	19.46	2.62
10	9.13	14.46	74.08	23.66	10.16	18.58	2.62
11	8.63	13.18	75.95	24.58	10.70	17.71	2.63
12	10.55	19.25	67.52	20.03	7.98	20.07	2.66
13	9.79	18.21	69.37	20.60	8.30	17.86	2.71
14	9.03	17.18	71.21	21.17	8.63	15.65	2.75
15	8.65	16.66	72.13	21.46	8.79	14.54	2.77
16	7.88	15.62	73.98	22.03	9.11	12.33	2.82
17	7.12	14.59	75.82	22.60	9.43	10.12	2.86
18	10.55	19.25	67.52	23.08	9.70	8.26	2.90
19	11.36	25.39	60.03	25.38	8.74	15.74	2.24
20	10.99	24.48	60.60	24.98	8.77	16.21	2.31
21	10.61	23.57	61.17	24.58	8.81	16.67	2.37
22	10.24	22.66	61.74	24.18	8.84	17.13	2.43
23	9.86	21.75	62.31	23.78	8.87	17.60	2.49
24	9.57	21.03	62.76	23.47	8.90	17.96	2.54
25	11.42	24.67	61.71	25.90	9.03	21.89	2.29
26	10.81	22.17	64.73	25.80	9.44	20.95	2.45
27	10.19	19.67	67.76	25.69	9.85	20.01	2.61
28	9.58	17.16	70.78	25.58	10.25	19.07	2.77
29	9.17	15.50	72.80	25.51	10.53	18.44	2.88
30	8.76	13.83	74.82	25.44	10.80	17.81	2.99
31	11.16	25.02	61.66	25.71	8.86	13.89	2.25
32	10.23	22.93	64.64	25.37	9.06	12.54	2.37
33	9.31	20.85	67.62	25.03	9.26	11.19	2.48
34	8.38	18.76	70.60	24.70	9.46	9.84	2.60
35	7.76	17.36	72.58	24.47	9.59	8.94	2.68
36	7.15	15.97	74.57	24.25	9.73	8.04	2.76
37	6.53	14.58	76.55	24.02	9.86	7.13	2.84
38	8.87	18.41	65.91	23.28	9.31	18.38	2.71
39	8.79	17.69	67.25	23.52	9.53	18.22	2.76
40	8.72	16.96	68.59	23.75	9.74	18.06	2.81
41	8.57	15.50	71.26	24.23	10.16	17.73	2.90
42	8.42	14.15	73.76	24.68	10.56	17.43	2.99
43	8.26	12.59	76.61	25.18	11.02	17.08	3.10
44	8.54	19.56	69.22	22.98	9.10	16.92	2.67
45	8.01	18.28	71.09	23.12	9.27	14.88	2.72
46	7.48	16.99	72.97	23.25	9.45	12.84	2.78
47	6.94	15.71	74.84	23.38	9.63	10.80	2.83
48	6.41	14.42	76.71	23.51	9.80	8.77	2.88
49	6.14	13.78	77.65	23.58	9.89	7.75	2.90

### 3. Establishment of Coke Quality Prediction Model

#### 3.1 Prediction Model Design

In this study, the BP neural network method was used to establish a coke quality prediction model. Before this, the input index was reduced by the principal component analysis method. To be able to verify the accuracy of the model, all sample data was divided into two groups: training samples and predictive samples [29]. Considering that the predictability of the model is closely related to the sample selected for training, in order to make the sample selection process balanced and representative, the five sets of single coal data are removed and the total sample is rearranged by the sort function to rearrange. The first 35 groups of post-data are used as training groups, and the last nine are used as prediction groups. The values of the coal blending parameters after dimension reduction are used as BP neural network inputs, and the measured values of CR, MSI, PRI and PSR are used as network outputs. Considering that it is better to convert a network model with multiple outputs into multiple network models with one output, and the training is more convenient [30].

Therefore, this study establishes four 4-input and one-output BP networks net1. -net4, the number of hidden layer nodes is determined to be 3, 5, 4 and 3, respectively. After setting the number of hidden nodes and network parameters, run the same network cycle for 100,000 times to save each training result and error. After completing all training, the net corresponding to the error value is defined as the optimal BP neural network.

### 3.2 Simulation Analysis of the Model

Based on the training results obtained in 3.1, nine sets of samples to be tested are input to the network. The network prediction results, experimental results and deviations are shown in Table 6.

Table 6 Comparison of measured and predicted values for coke quality

No.	<i>CR</i>		<i>MSI</i>		<i>PRI</i>		<i>PSR</i>	
	measured	prediction	measured	prediction	measured	prediction	measured	prediction
	deviation /%		deviation /%		deviation /%		deviation /%	
41	65.70	65.90	36.04	37.43	58.20	57.48	17.30	18.81
	-0.30		3.86		1.24		-8.73	
42	72.83	72.62	45.70	46.12	53.13	53.00	51.78	48.58
	0.29		-0.92		0.24		6.18	
43	72.50	72.21	45.03	45.38	58.06	58.13	35.96	34.85
	0.40		-0.78		-0.12		3.09	
44	61.93	62.63	33.51	33.95	59.50	59.75	22.37	18.78
	-1.13		-1.31		-0.42		16.05	
45	69.77	69.47	48.02	47.89	59.32	61.18	40.63	43.62
	0.43		0.27		-3.14		-7.36	
46	71.55	70.78	48.73	48.83	62.84	64.36	25.12	20.49
	1.08		0.21		-2.42		18.43	
47	70.94	70.88	50.95	51.57	59.03	60.54	37.81	34.91
	0.08		1.22		-2.56		7.67	
48	65.03	64.76	39.81	38.74	57.35	57.97	14.97	18.81
	0.42		2.69		-1.08		-25.65	
49	71.88	72.36	39.71	40.87	71.66	71.43	20.40	23.84
	-0.67		2.92		0.32		-16.86	
Mean deviation /%	0.53		1.58		1.28		12.22	
Maximum deviation /%	1.13		3.86		3.14		25.65	

<sup>a</sup> : deviation =( measured value-prediction value) / measured value

In order to more intuitively express the prediction accuracy of the model, the allowable relative errors are set to 10%, 5%, 4% and 3% respectively to examine the hit rate of the model for the predicted samples. The results are shown in Table 7.

For example, when the relative error is allowed to be 5%, the predicted effect diagram is shown in Fig. 3. In Fig. 3, the solid line equation is  $y=x$ , which indicates that the predicted value of the model is equal to the measured value; the two dotted equations are  $y=x+0.05x$  and  $y=x-0.05x$ , respectively. The allowed range. Within the dashed line range (including the points in the line) , but for points which are not within the dashed line range, the prediction fails.

From Table 6, Table 7, and Figure 3, the model has the best predictive power for CR. The average deviation of nine points is only 0.53%. When the relative error is 2%, the hit rate is still 100%, that is, the model is CR. The prediction accuracy is above 98%; the prediction ability for MSI and PRI is also good, the average deviation is 1.58% and 1.28%, respectively, and the relative error is 4%, the hit rate is 100%, while allowing relative error is 3%, the hit rate is 88.89%. It can be seen that the prediction accuracy of the model for MSI and PRI is above 96%; the prediction ability for PSR is poor. The average deviation of nine samples is 12.22%, allowing relative error. At 10%, the hit rate is only 55.56%, and when the relative error is 5%, the hit rate drops to 11.11%. In addition, the predicted and measured values of each index are linearly regressed by  $y=x$ , and their  $R^2_{adj}$  values are 0.987, 0.982, 0.956, and 0.926, respectively, indicating the prediction of CR, MSI, PRI, and PSR. There is good consistency between the value and the measured value.



Table 7 Hit rate of coke quality under different allowed relative errors

Allowed relative error /%	CR hit rate /%	MSI hit rate /%	PRI hit rate /%	PSR hit rate /%
10	100	100	100	55.56
5	100	100	100	11.11
4	100	100	100	11.11
3	100	88.89	88.89	0
2	100	66.67	66.67	0

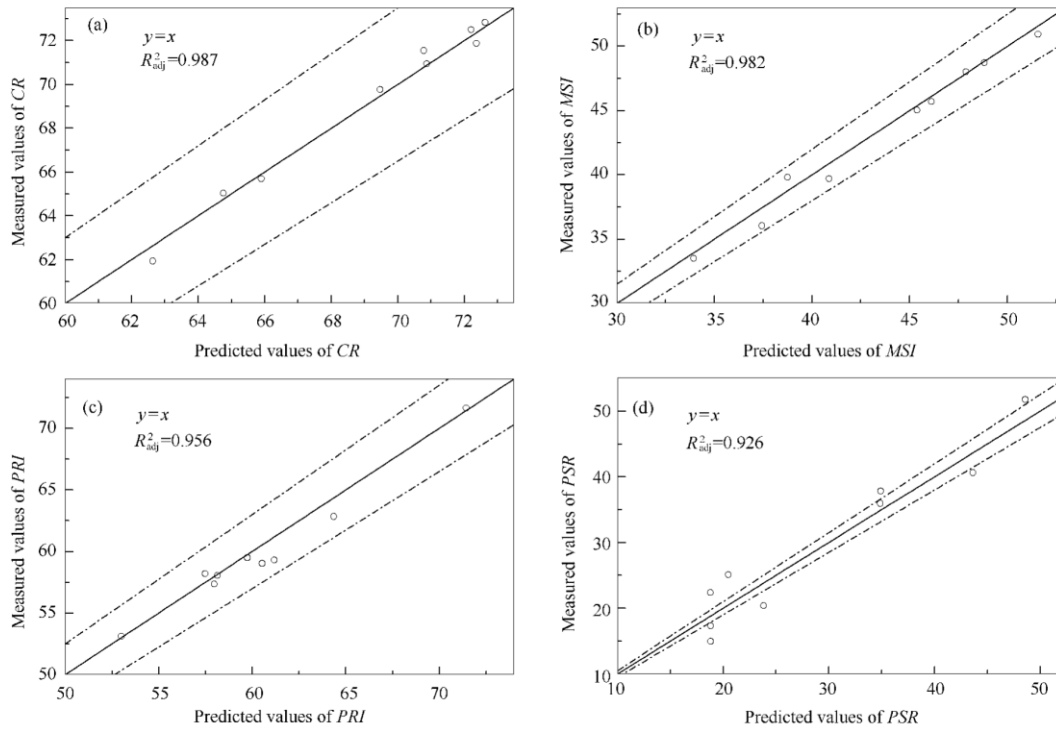


Figure 3 allows the prediction effect when the relative error is 5%

### 3.3 Discussion of the Model

Guo Yinan et al.<sup>[31]</sup> used a hybrid algorithm to establish a coke quality prediction model with Ad, Vdaf, St, d and G, and predicted the prediction accuracy of coke M40, M10, ash and sulfur by 95%-97%; Zhou Hong et al.<sup>[15]</sup> used the BP neural network method to predict coke M40, M10, ash and sulfur with G, Vdaf, St, d and Ad as coal blending indexes, and the hit rate reached 94% when the relative error was 5%. Hu Desheng et al.<sup>[32]</sup> Predict the DI1550, CRI and CSR of coke by using the total content of inert matter TI, Vd and the comprehensive bond index CCI (calculated from G, Kjeldahl MF and vitrinite bond index VCI, expressing the characteristics of actives in coal). Through the 20kg small coke oven experiment, the linear fitting R2 coefficients of the predicted and actual values obtained by the regression ternary cubic equation are 0.962, 0.905 and 0.917, respectively; Zhang Qun et al.<sup>[9]</sup> are inert Content TI, random reflectance R, bond index G, basic fluidity MF and mineral catalytic index MCI are coal blending indicators. The  $G_{MDH}$  data processing method is used to establish a coke quality prediction model for SCO furnaces, with DI1550, CRI and CSR. The correlation coefficient  $r$  between the predicted value and the measured value for  $y=x$  is 0 respectively. 76, 0.86 and 0.88; lvarez et al.<sup>[4]</sup> proposed a method for calculating the mass of coal coke by using the mass of single coal coke, and found that the prediction ability of coke cold strength is poor, but CRI and CSR have good predictive power, and the hit rate can reach 100% with an allowable error of 2.8% and 5.4%, respectively.

It can be seen that in addition to the traditional experience of blending coal and coal blending, people are still researching and pursuing the use of new coal blending indicators to establish a coke quality prediction model. The traditional Ad, Vdaf, St, d and G are used as coal blending indexes. Generally, only the cold properties of coke, such as M40 and

M10, have good predictive ability; while the comprehensive application of G, Vd, and basic fluidity MF And the new coal blending index of coal rock characteristic parameters, the cold and hot properties of coke such as DI11550, CRI and CSR have certain predictive ability.

This study is based on the coke property indicators MSI, PRI and PSR used in laboratory research. It is different from the industrial use of DI11550, CRI and CSR indicators, but has corresponding correspondence, which also reflects the cold strength and heat of coke. Reactivity and post-reaction strength. From the results of the model alone, the R<sup>2</sup> of the linear regression of the predicted and measured values of the indicators in this study is significantly higher than that of Zhang Qun et al. [9], and the results of Hu Desheng et al. [32] (not the linear fit of  $y=x$ ) is also slightly better. Explain that the coal blending parameters selected in this paper have certain advantages.

In fact, Zhang Qun et al [9] and Hu Desheng et al [32] in the coal blending parameters have chosen coal rock indicators, including inert content TI, random reflectivity R, vitrinite bond index VCI. These indicators reflect the content and characteristics of actives and inerts in coal to a certain extent. It can be said that it is a coal blending coking prediction method based on the active components and inert components of the lithofacies. Because this method takes into account the problem of active and inert components in coal, it also reflects the compositional nature of coal to a certain extent, so that the thermal properties of coke can be correlated. However, the above coal rock index can only be used as a reflection of the different structural structures in the lithofacies of coal, but it is not the essence of coal composition.

The I3 and I4 indicators selected in this study are based on the FT-IR analysis of coal. The expression of the functional group content in the coal structure directly reflects the structural nature of the coal. At the same time,  $Y_{DMC}$ ,  $Y_{LMC}$  and YHC are selected. The non-lithographic angle directly expresses the content of active and inert components in coal, and also reflects the fluidity and swelling ability of coal pyrolysis. Therefore, the I3, I4,  $Y_{DMC}$ ,  $Y_{LMC}$  and YHC indicators selected in this study can reflect the inert content TI, random reflectivity R, and mirror in the method of Zhang Qun et al [9] and Hu Desheng et al. [32]. The mass group adhesion index VCI and the characteristics of the raw coal G value and the basic fluidity MF can reflect the essence of the coal structure, so it should be one of the many advantages of many coal blending parameters.

In addition to Ad and Vdaf, the other parameters of coal blending selected in this study are the new indicators of I3, I4,  $Y_{DMC}$ ,  $Y_{LMC}$  and YHC, and these five new indicators are the original structure and composition of raw coal. The parameter is a parameter that has not undergone any thermal change. It is a parameter of the "non-nature" aspect of coal and belongs to the "compositional structural parameter" of coal. Ad and Vdaf are parameters of coal after heat treatment, reflecting the nature of coal. It belongs to the "property parameter" of coal. It can be seen from the above discussion that the traditional coal blending parameters only use the "property parameters", that is, the coke quality prediction model is mainly established by Ad, Vdaf, St, d and G; the coal blending method integrating the coal rock parameters is only used in a small amount. "Compositional structural parameters" such as inert content TI and random reflectance R, and mainly used are "property parameters", including Vd, G, MF, vitrinite group adhesion index VCI and mineral catalytic index MCI. Therefore, this study establishes a new coke quality prediction model based on coal "compositional structural parameters", which is also the largest and most core feature of this model.

However, Table 7 also shows that although the predicted and measured values of the PSR in this model are still in good agreement with the linear relationship of  $y=x$ , the error is significantly larger, for example, when the relative error is allowed to be 10%, the hit rate is only It is 55.56%. This is because the coke obtained in this experiment belongs to highly reactive coke (PRI data of Table 7), and the main component of the carbon residue after the reaction is an inorganic component (various inorganic oxides), and therefore, the quality and quantity of the inorganic component. It should have an important impact on the PSR. Related studies have applied the quality and quantity of inorganic components to the prediction of strength after coke reaction [9, 33, 34] and achieved good results. In fact, for highly reactive coke, it is not appropriate to evaluate the post-reaction strength with PSR or CSR. Nomura et al. [35] discussed this and considered that the post-dissolution strength of highly reactive coke should be evaluated by the method of 20% fixed weight loss rate and changing reaction temperature to adjust the reaction rate, and evaluated under the condition of equal dissolution rate. The post-reaction strength of coke can eliminate the effects of coke reactivity.

## 4. Analysis of Coke Forming Mechanism under the New Model

The above-mentioned new model of coke quality prediction based on coal non-lithographic phase active/inert component separation and characterized by “coal compositional structural parameters” must have its coke formation mechanism. In order to investigate the coking mechanism, the morphological changes of DMC, LMC, HC and LC components in the process of heated carbonization were investigated. Except for LC, each group of components was pressed into a circular piece having a diameter of about 10 mm and a thickness of about 1 mm under a pressure of 5 MPa. The components of each group were placed in a constant temperature zone of a tube furnace through N<sub>2</sub>, and the temperature was raised to 600 °C at a constant rate of 5 °C / min, and the changes during the process were observed and recorded at any time.

### 4.1 Changes in the Heat Form of Each Family Component

Figure 4 shows the process of changing the heat form of DMC. At 200 °C, DMC begins to soften and expand into a hemispherical shape. The surface of the hemisphere is smooth and free of pores. At 220-240 °C, with the increase of softening degree, the hemisphere is soft and the bottom area is increased and the height is lowered. At 250 °C, gas begins to flow. The surface escapes and produces small pores, while the bottom area is further increased; at 250-300 °C, the amount of pores on the surface is more and more, and the flowing liquid phase is generated at 310-330 °C, and the bottom area is rapidly expanded; after 340 °C, the amount of liquid phase formation is increasing, and gradually dominates the deformation and flow of DMC, but the amount of gas generated is not significant; until 380 °C, the amount of gas generated is significantly increased, the pyrolysis reaction is intense, the surface is interwoven with bubble generation and during the rupture, the bottom area is also basically increased to the maximum; thereafter, the state is maintained substantially until 430-460 °C, the gas generation amount is significantly reduced; however, after 470 °C, more and larger bubbles are generated, but the bubble cracking rate is obviously less than 380-415 °C; at 500 °C, it can be clearly observed that the liquid phase begins to solidify; the liquid phase disappears at 540 °C, and substantially solidifies to form semi-coke.

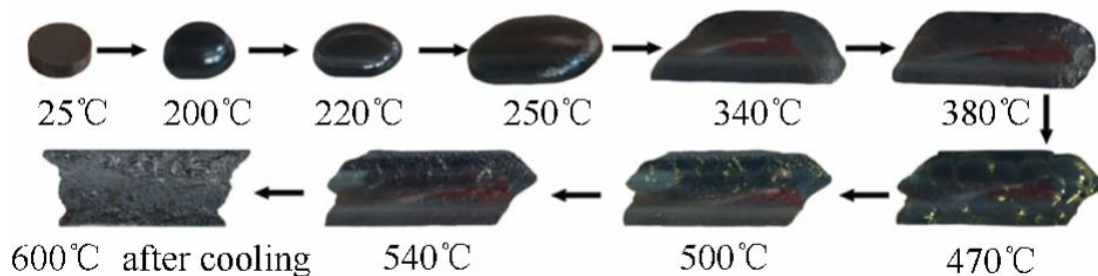


Figure 4: Thermal changes in DMC pellets at different temperatures

Figure 5 shows the process of changing the morphology of the LMC. Before 430 °C, LMC maintains the shape of the wafer; at 440 °C, the visible expansion phenomenon begins to appear, some of the gas escapes and produces pores on the surface, and no visible softening phenomenon is observed (but there is a softening and melting process); 440-460 °C, LMC is in a sharp expansion phase, the pyrolysis reaction is intense; 460-500 °C, into the slow expansion phase; 500-600 °C, the formation of semi-coke and the volume almost no change.

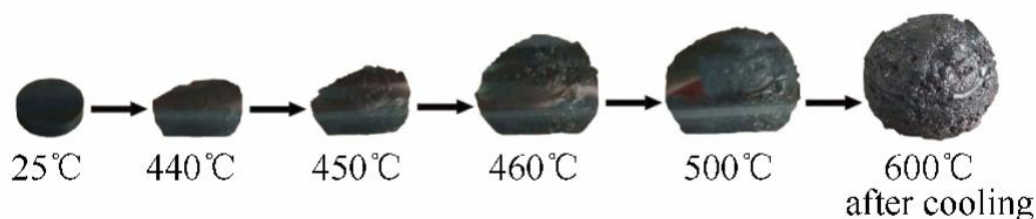


Figure 5: Changes in the heat form of LMC pellets at different temperatures

Figure 6 shows the change in the heating pattern of HC. There was almost no morphological change in the whole process of HC, and the original wafer form and size were completely maintained after 600 °C. Figure 7 shows the change in the heat form of the LC. At 180 °C, the LC begins to soften and swell; at 240 °C, gas is generated and escapes from the softened surface, but the amount of gas generated before 260 °C is small, and the bubbles are small; at 260 °C, the LC produces a liquid phase and begins to flow. At this time, the decomposition is intensified, and the amount of bubbles is increased; 260-360 °C, maintaining rapid decomposition state, the bubbles are large and large, and the flow range is slightly increased; at 380 °C, the decomposition rate is slowed down, and few new macroscopic bubbles are generated; 480 °C, liquid phase solidification, cracks on the surface; 480-600 °C, complete curing, a large number of cracks on the surface. The char formed by LC is actually a blister-like hollow structure, the bubble wall is very thin and brittle, and the yield is only 35.93%.

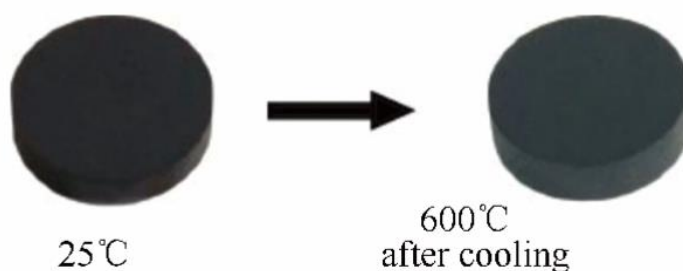


Figure 6 shows the change of the heating shape of the HC tablet at different temperatures.

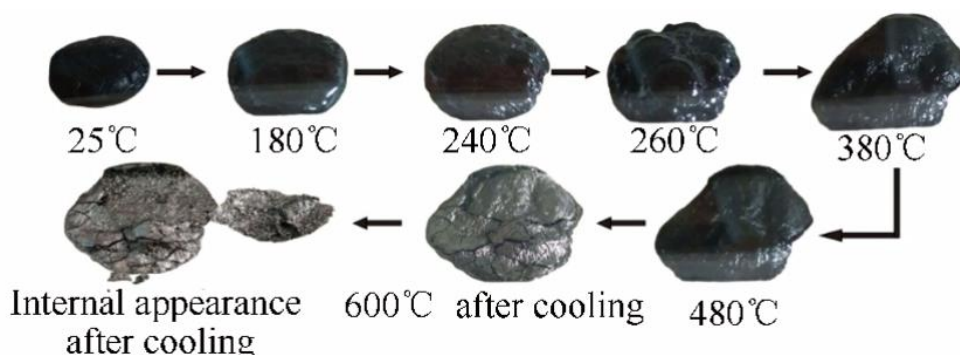


Figure 7 shows the change of the heating state of the LC at different temperatures.

The above situation indicates that there are significant differences in the pyrolysis behavior and the change in the heating form of the four major components of DMC, LMC, HC and LC. It is quite obvious that DMC provides a source of fluidity (liquid phase) during pyrolysis of coking coal, LMC provides a source of swelling (gas phase and melting)

during pyrolysis, and HC provides solid-source properties during pyrolysis. The source of (sand) LC is weak due to its low content in coal.

## 4.2 Coke Forming Mechanism under the New Model

According to the theory of coal inlay structure model created by the extraction and extraction method to achieve the separation of coal components [36], the above three components of DMC, LMC and HC are particles of 120, 80-100 and 50-80 nm, respectively. The mutual embedding constitutes the coal as a whole, and the lightweight group LC acts as a bridge connecting the particles. Among them, the DMC particles are formed by agglomerating agglomerates of 5 nm nanoparticles and then superimposing and agglomerating. In coking coal, DMC generally accounts for 5%-15%, LMC generally accounts for 10%-30%, and HC generally accounts for 50%-80%.

Thus, the coking coal coking process can be divided into the following six stages: room temperature -200 °C, drying stage; 200-340 °C, DMC deformation stage; 340-440 °C, DMC liquid phase and flow filling void stage; -500 °C, LMC produces expansion to form bubbles and thin walls, thin wall is subjected to extrusion and continuous rupture stage, wherein 440-460 °C is the rapid expansion stage, 460-500 °C is the slow expansion stage; 500-540 °C, solidification is half Focal stage; 540-1000 °C, semi-coke shrinkage becomes the stage of coke.

Fig. 8 is a schematic diagram showing the coking mechanism of coking coal having different contents of two kinds of components, wherein the coking coal DMC content of Fig. 8(a) is higher, and the coking coal DMC content of Fig. 8(b) is lower. It can be seen from Fig. 8(a) that from 200 °C, the DMC particles embedded in the coal soften and deform, and gradually penetrate into the peripheral particle voids, but the permeability is poor; until the 340 °C DMC becomes liquid phase, When the flow phenomenon occurs, the liquid phase easily invades into the surrounding space and gradually fills the corresponding voids. At this time, there is no obvious morphological change of LMC and HC particles, and the whole coal particles remain basically unchanged in the original external shape; at 440 °C, DMC The liquid phase not only fills all the voids of the entire coal particles, but even reaches the surface of the coal particles, forming a state in which the LMC and HC particles are completely surrounded by the DMC liquid phase; At the beginning of this temperature, the LMC melts and rapidly undergoes a pyrolysis reaction, and a large amount of gas is generated to rapidly expand the LMC particles. At the same time, due to the surrounding DMC liquid phase surrounding, the expansion capacity is further increased, and the overall coal particle volume is increased; at 460 °C, the thin wall of the LMC particles formed by the expansion of LMC produces cracks, from which the gas escapes and passes through the DMC liquid phase in the gap to the surface of the coal particles; thereafter, the expansion process becomes slow until 500 °C; both the DMC liquid phase and the thin walls of the LMC enter the solidification stage, and they enclose the HC particles which form only a small amount of gas and whose morphology is substantially unchanged to form a semi-coke. Since the liquid phase of the DMC is more wrapped in place, the formed semi-coke strength is higher.

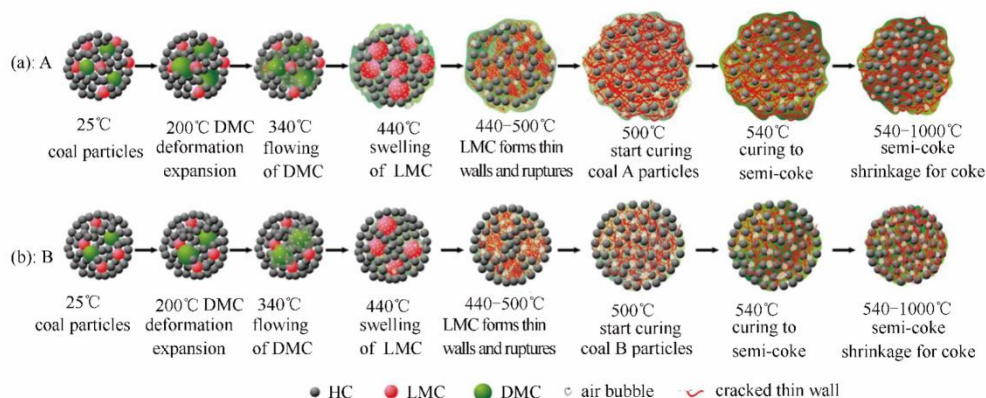


Figure 8 shows the coking mechanism of two types of coking coal (inside the coal particles)

For the coking coal B of Fig. 8(b), since the DMC content is small, the generated DMC liquid phase is insufficient to fill all the voids in the coal particles, and thus the complete wrapping of the LMC rupture thin wall and the HC particles



cannot be formed, and thus It is much easier to escape the coal particles during the process, and the expansion of the coal particles is relatively small; in particular, less DMC liquid phase can not achieve effective encapsulation of HC particles, therefore, the semi-coke generated by B coking coal. The intensity is significantly lower.

The above is based on the mechanism analysis of a coal particle of a single coking coal (such as the coal particles  $\leq 1.6\text{mm}$  used in this experiment). It is discussed that the coal particles are self-focusing and embedded inside. The coke behavior of DMC, LMC and HC of cloth. Then, when these coal particles are mixed together, how do they form coke blocks?

Figure 9 shows the coking process between coal particles during coking coal A with high DMC content.

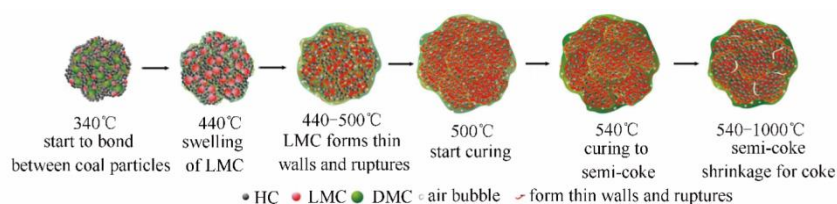


Figure 9 Single coal coking mechanism (coking coal A, between coal particles)

From the previous analysis, at this time, the DMC liquid phase can reach the surface of the individual coal particles, and at the same time, the good expansion property causes the individual coal particles to approach each other and adhere, thereby bonding the individual coal particles to each other and solidifying block semi-coke. The final coke produced by this semi-coke has a higher strength. However, if the coking coal B with a lower DMC content is separately coked, it can be seen from the previous analysis that the surface of the individual coal particles cannot be wrapped by the liquid phase at the same time, and the swelling property is relatively poor, so that it is difficult to achieve good between the individual coal particles. Adhesive, naturally solidified semi-coke is difficult to block or block strength is low.

However, if coking coal B containing more DMC is blended in coking coal B, see Figure 10 for details. At this time, the single coking coal A particles having a DMC liquid phase on the surface will adhere to the coking coal B particles having no surface liquid phase through the liquid phase, thereby achieving mutual adhesion of the two coal particles to a certain extent. If the blending amount is appropriate, it is also possible to produce semi-coke and coke of appropriate strength. However, when using coal blending, it is necessary to thoroughly mix the coal particles of the two coal types. Otherwise, the generated semi-coke or coke may cause local unevenness.

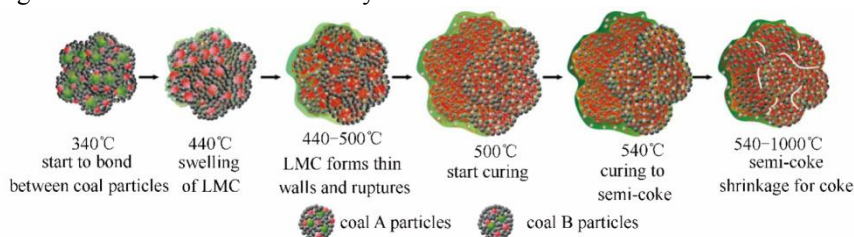


Figure 10: Coking mechanism of coal blending (between coking coal A and coking coal B particles)

## 5. Conclusion

Separation of coal components into coal heavy group HC, dense medium group DMC and thin medium group LMC and other components, is a new method for non-rock phase separation of coking coal and inert components. From the yields of these components, YHC, YDMC, YLMC, and parameters such as I3 and I4 reflecting the hydrogen bond association characteristics and aliphatic structural characteristics in coal, the coke quality can be effectively predicted. These new parameters reflect the chemical composition and structural nature of coal, and belong to the “compositional structural parameters”. It is completely different from the “property parameters” in the traditional coke prediction method, and it



has certain advantages to establish a coke quality prediction model.

The coke quality prediction model established by the "structural parameter" and BP neural network method has higher prediction accuracy for the focal rate CR, microscopic intensity MSI and particle coke reactivity PRI. CR, MSI of nine predicted samples deviation from PRI is 0.53%, 1.58%, and 1.28%, respectively, where the prediction accuracy of CR is above 98%, and the prediction accuracy of MSI and PRI is above 96%; CR, MSI, and PRI The correlation coefficients of the predicted and measured values for  $y=x$  are 0.987, 0.982 and 0.956 respectively; however, the prediction effect on the intensity PSR after the reaction is poor, and the PSR of the nine predicted samples. The average deviation is 12.22%, but the correlation coefficient between the predicted and measured values for  $y=x$  still reaches 0.926.

The pyrolysis behavior and the change of the heated form of the group components DMC, LMC, HC and light group LC have significant differences. Among them, DMC provides the source of fluidity (liquid phase) in the pyrolysis process of coking coal, and LMC provides heat. The source of swelling (gas phase and melting) during the solution process, HC provides a source of solid-source (sand) in the pyrolysis process. LC is weak due to its low content in coal.

The coking coal coking process consists of six main stages: room temperature -200 ° C, drying stage; 200-340 ° C, DMC deformation stage; 340-440 ° C, DMC produces liquid phase and produces a flow-filled void stage; 440-500 ° C, LMC Produces expansion to form bubbles and thin walls, and the thin wall is subjected to extrusion and continuous rupture stage, wherein 440-460 ° C is a rapid expansion phase, 460-500 ° C is a slow expansion phase; 500-540 ° C, solidification is a semi-coke phase; 540- At 1000 ° C, the semi-coke shrinkage becomes the stage of coke.

This study explored the coking mechanism of coking coal under the coke quality prediction model, and provided a basis for establishing a new coking coal blending method based on "compositional structural parameters".

## Acknowledgement

Jiangsu Yinzhou Coal Coking Co., Ltd. provided coking experimental conditions for this study. Sun Zhang, graduate student of the School of Chemical Engineering, North China University of Science and Technology, and post graduate Duan Chong provided assistance in the test of particle coke reactivity.

## References

1. Xie Haishen, Liu Yongxin, Lu Qing, Meng Junbo Coke quality prediction model [J] Journal of Northeastern University (Natural Science Edition), 2007, 28(3): 373-377
2. D EZMA, ALVAREZR, BARRIOCANALC. Coal metallurgy technology production: manufacturing quality forecast and future demand forecast [J]. Int J Coal Geol, 2002, 50 (1/4): 389-412.
3. ZHANGQ, WUX, FENGA, SHIM. Baosteel's fair quality prediction [J] . FPT, 2004, 86 (1): 1-11.
4. LVAREZR, D EZMA, BARRIOCANALC, D AZ-FAESE, CIMADEVILLAJLG. An approach to blast furnace coke quality prediction [J]. Fuel, 2007, 86 (14): 2159 to 2166.
5. MORGAR, JELONEKI, KRUSZEWSKAK, SZULIKW. Neutral relationship, resulting in results and microscopic tensile spectral features [J]. IntJCoalGeol, 2015, 144 / 145: 130-137.
6. CHEHREHCS, MATINSS, HOWERJC. The relationship between quality indicators and coal properties was explained by random forest method [J]. Fuel, 2016, 182: 754-760.
7. YUAB, STANDISHN, LUL. Coagulation and density effects on density [J]. Powder Technol, 1995, 82(2): 177-189.
8. NOMURAS, THOMASKM. The effect of environmental pressure coal carbonation on porosity [J]. Fuel, 1996, 75(2): 187-194.
9. Zhang Qun, Wu Xinyu, Feng Anzu, Shi Meiren. Baosteel coke quality prediction model II. The establishment and application of coke quality prediction model [J]. Journal of Fuel Chemistry, 2002, 30(4): 300-305.
10. Wang Guanghui, Fan Cheng, Tian Wenzhong, Yu Mingcheng, Liu Zhiping, Pan Lihui, Yan Meicheng. Research on coke quality prediction method [J]. Journal of Wuhan University of Science and Technology (Natural Science Edition), 2007, 30(1): 37-40.
11. Lu Guishuang, Zheng Meirong, Zhao Hua, Chen You. Factors affecting coke reactivity and post-reaction intensity [C]. National Steel Production Technology Conference and Ironmaking Academic Annual Conference, 2009.
12. Zhou Shiyong. Application of coal rock science [M]. Beijing: Metallurgical Industry Press, 1985.
13. Zhou Shiyong, Zhao Junguo. Metallurgical Industry Press, 2005.

14. Yang Jiangang. Artificial neural network practical tutorial [M]. Hangzhou: Zhejiang University Press, 2001.
15. Zhou Hong, Yan Lishu, Zou Xianglin. Prediction of coke quality in extra large coke oven based on neural network [J]. Journal of System Simulation, 2009, 21(6): 1543-1547.
16. Liu Jun, Zhang Xuedong, Liu Hong, Xu Haiping. Prediction of coke quality based on BP neural network [J]. Fuel and Chemical Engineering, 2006, 37(6): 12-15.
17. Jiang Jing, Gong Chunhui. Application of neural network in coke quality prediction model [J]. Journal of Shenyang Ligong University, 2013, 32(2): 25-27.
18. Qin Zhihong, Li Xingshun, Chen Juan, Zhang Liying, Hou Cuili, Gong Tao. Coal bonding source and formation mechanism [J]. Journal of China University of Mining and Technology, 2010, 39(1): 64-69.
19. Li Xiang, Qin Zhihong, Bu Lianghai, Yang Zhe, Shen Chenyang. Structural analysis of coking coal functional group and its bonding production mechanism [J]. Journal of Fuel Chemistry, 2016, 44(4): 385-393.
20. QINZ, HOUC, CHENJ, ZHANGL, MAJ. Group separation of coal components and new ideas of coal utilization as petroleum [J]. Int J Min Technol, 2009, 19(5): 636-641.
21. QIX, WANGD, XINH, QIG. Study on real-time changes of anaerobic reactive groups in coal [J]. EnergyFuels, 2013, 27(6): 3130-3136.
22. Sun Zhang, Guo Rui, Liu Pengfei, Liang Yinghua. The relationship between particle coke dynamic reactivity and block coke reactivity [J]. Coal Conversion, 2015, 38(3): 70-73.
23. Yang Junhe, Du Hegui, Qian Zhanfen, Cui Ping. Coke reactivity of coke [J]. Journal of Northeastern University, 1999, 20(3): 64-67.
24. PRICEJT, KHANMA, GRANSDENJF. The "Supper coke" from the western coast of Canada has a high strength [C]. 59th Iron making Conference Proceedings. Chicago, Illinois, 1999: 227-239.
25. Zhang Qun, Wu Xinxu, Feng Anzu, Shi Meiren. Baosteel coke quality prediction model I. Factors affecting coke thermal performance [J]. Journal of Fuel Chemistry, 2002, 30(2): 113-118.
26. QINZ, LIX, SUNH, ZHAOC, RONGL. Caking property and active components of coal based on group component separation [J]. Int J Min Technol, 2016, 26(4): 571-575.
27. Zhang Shuangquan. Coal Chemistry [M]. Xuzhou: China University of Mining and Technology Press, 2009.
28. Weng Shizhen. Fourier transform infrared spectrometer [M]. Chemical Industry Press, 2005.
29. Zhang Defeng. MATLAB neural network application design [M]. Beijing: Mechanical Industry Press, 2009.
30. Wang Xiukun, Zhang Xiaofeng. Replace the multi-output BP network with a set of single output subnets [J]. Computer Science, 2001, 28(10): 61-63.
31. Guo Yinan, Wang Ling, Tan Dejian, Hao Hao. Coal blending control based on genetic algorithm and neural network hybrid optimization [J]. Journal of China University of Mining and Technology, 2002, 31(5): 404-406.
32. Hu Desheng, Wu Xinyu, Dai Chaofa. Baosteel coke strength prediction and coal quality control [J]. Bao steel Technology, 2000 (3): 30-34.
33. GOSICINSKIJS, GRAYRJ, ROBINSONJW. US coal quality assessment and reaction intensity and reaction intensity after impact reaction [J]. J Coal Quality, 1985, 4(2): 35-43; 4(4): 21-29.
34. VALIAHS. The reaction of CO<sub>2</sub> from the reaction of coal analyses at inlands company was predicted [J]. Iand SM, 1989, (5): 77-87.
35. NOMURAS, NAITOM, YAMAGUCHIK. After the reaction intensity, the catalyst is added to a highly reactive reaction [J]. ISIJ Int, 2007, 47(6): 831-839.
36. Qin Zhihong. Coal inlay structure model theory [J]. Journal of China University of Mining and Technology, 2017, 46(5): 939-958.